Eur. Phys. J. E (2014) **37**: 69
DOI 10.1140/epje/i2014-14069-2

THE EUROPEAN PHYSICAL JOURNAL E

Regular Article

Elasticity and mechanical instability of charged lipid bilayers in ionic solutions

Yotam Y. Avital[1,2], Niels Grønbech-Jensen[3,4], and Oded Farago[1,2,a]

[1] Ilse Katz Institute for Nanoscale Science and Technology, Ben Gurion University of the Negev, Be'er Sheva, 84105, Israel
[2] Department of Biomedical Engineering, Ben Gurion University of the Negev, Be'er Sheva, 84105, Israel
[3] Department of Mechanical and Aerospace Engineering, University of California, Davis, CA 95616, USA
[4] Department of Mathematics, University of California, Davis, CA 95616, USA

Received 4 May 2014 and Received in final form 29 June 2014
Published online: 15 August 2014 –

Abstract. We use coarse-grained Monte Carlo simulations to study the elastic properties of charged membranes in solutions of monovalent and pentavalent counterions. The simulation results of the two cases reveal trends opposite to each other. The bending rigidity and projected area increase with the membrane charge density for monovalent counterions, while they decrease for the pentavalent ions. These observations can be related to the counterion screening of the lipid charges. While the monovalent counterions only weakly screen the Coulomb interactions, which implies a repulsive Coulomb system, the multivalent counterions condense on the membrane and, through spatial charge correlations, make the effective interactions due to the charged lipids attractive. The differences in the elastic properties of the charged membranes in monovalent and multivalent counterion solutions are reflected in the mechanisms leading to their mechanical instability at high charge densities. In the former case, the membranes develop pores to relieve the electrostatic tensile stresses, while in the latter case, the membrane exhibits large wavelength bending instability.

1 introduction

Lipid bilayers are fundamental to all living cells and participate in diverse biological processes [1]. Their elasticity is traditionally treated withing the framework of the Helfrich effective Hamiltonian relating the elastic energy density (per unit area $\mathrm{d}S$) of a thin sheet to the local principle curvatures c_1 and c_2 [2]

$$\mathcal{H} = \int_S \left[\gamma + \frac{1}{2}\kappa\left(c_1 + c_2 - 2c_0\right)^2 + \kappa_G c_1 c_2\right] \mathrm{d}S, \qquad (1)$$

where γ, κ, and κ_G denote the surface tension, bending rigidity, and saddle-splay modulus, respectively, and c_0 is the spontaneous curvature. The elastic moduli appearing in eq. (1) are primarily governed by the short-range intermolecular forces between the lipids [3]. Biological membranes, however, are often charged and suspended in ionic solutions, and the long-range electrostatic interactions are expected to contribute to κ and κ_G. Solutions of the Poisson-Boltzmann (PB) equation for spherical, cylindrical, and sinusoidal geometries suggest that κ increases with the surface charge density [4]. This trend of increase in κ, predicted by the mean-field theory, holds true for both weak and strong electrolytes, irrespective of the degree of electric coupling between the two monolayers. Going beyond mean field, by considering charge density fluctuations and their spatial correlations, has led to several opposing predictions that κ may be reduced in the presence of charges [5–8]. Spatial charge correlations effects (which are missing in the mean-field description) become significant when bilayer membranes are suspended in solutions with multivalent counterions [9,10]. The phenomenon most associated with these effects is the attraction between similarly charged objects [11–13], which is found in many biological systems, *e.g.*, in cell-cell adhesion and DNA condensation. The reduction in κ of bilayer membranes is a less commonly recognized phenomenon involving both charge-charge and *height-charge* correlations. The details of this effect are not fully understood, but it is generally believed to be small and, thus, hard to measure experimentally. Also, the attractive electrostatic interactions between multivalent counterions, which presumably lead to a decrease in κ, may be overshadowed by other intermolecular interactions, especially when screened by added salt. It has, in fact, been suggested [5,8] that when the Debye screening length falls below the typical spacing between the multivalent counterions, the change in κ becomes positive rather than negative (as predicted by mean-field theory). Here, we approach this topic through computer simulations of fluctuating bilayers, which allow

[a] e-mail: ofarago@bgu.ac.il

us to explore the effect in the absence of added salt and other influences. Our results support the picture that spatial correlation in the charge density due to the presence of highly multivalent counterions tend to soften membranes and reduce their bending rigidity. To the best of knowledge, this is the first simulation study to report this phenomenon, with the exception of the work of Fleck and Netz [14] who investigated the enhancement of short wavelength protrusion modes (to be distinguished from the long-wavelength bending modes discussed here) due to electrostatic repulsion between the membrane charges.

The bending modulus of symmetric bilayers ($c_0 = 0$ in eq. (1)) can be derived by considering the Fourier space representation of the Helfrich effective Hamiltonian. For a weakly fluctuating membrane, the surface S can be described within the Monge gauge by the height function $h(\vec{r})$ above a square flat reference surface of linear size L. Upon introducing the Fourier transform of $h(\vec{r})$: $h_{\vec{q}} = (l/L)\sum_{i=1}^{(L/l)^2} h(\vec{r}_i)e^{i\vec{q}\cdot\vec{r}}$, where the sum runs over a set of $(L/l)^2$ grid points at which $h(r)$ is evaluated (with l being a microscopic cutoff length of the order of the width of the bilayer), and $\vec{q} = (2\pi/L)(n_x, n_y)$ is the wave vector with $n_{x,y} = -L/l, \ldots, -1, 0, 1, \ldots, L/l$, the Hamiltonian decouples into a sum of independent harmonic oscillators. Applying the equipartition theorem to each Fourier mode, one finds that

$$\left\langle |h_{\vec{q}}|^2 \right\rangle = \frac{k_B T L^2}{l^4(\gamma q^2 + \kappa q^4)}\,, \tag{2}$$

where k_B is Boltzmann constant and T is the temperature. The accuracy of eq. (2) has been demonstrated in numerous atomistic and coarse-grained (CG) bilayer simulations (see, *e.g.*, [15–18]). Because this result is based on a quadratic approximation of eq. (1), it is strictly valid only for moderately fluctuating surfaces, *i.e.*, for $|\vec{\nabla}h(\vec{r})| \ll 1$. Here we demonstrate that charged membranes in solutions of pentavalent counterions exhibit strong thermal height fluctuations, and tend to develop long-wavelength bending instabilities. Membrane in solutions of monovalent counterions do not exhibit this type of behavior, but rather become mechanically unstable through a surface-tension-type mechanism.

To allow for simulations of relatively large membranes, we use Deserno's implicit-solvent model [19], where each lipid is represented as a trimer consisting of one hydrophilic (head) and two hydrophobic (tail) beads of size σ. We set the parameters of the hydrophobic pair potential to $\epsilon = 1.05k_BT$ (potential depth) and $w_c = 1.35\sigma$ (potential range). This choice yields remarkably soft membranes with bending rigidity $\kappa \simeq 8k_BT$, which is an essential property for this study since the electrostatic contribution to κ is expected to be small and difficult to measure ($|\delta\kappa| \simeq k_BT$). We convert a fraction ϕ of the neutral lipids to anionic lipids by introducing a charge of size $-e$ at the center of their head beads. The negative charges of the lipids are neutralized by either monovalent or pentavalent counterions, with no added salt. In physical units $\sigma \simeq 6.5\,\text{Å}$, corresponding to a bilayer of thickness $2 \times 3\sigma \sim 4\,\text{nm}$. Setting the temperature to 300 K implies that the Bjerrum length $l_B \simeq 7.1\,\text{Å} \simeq 1.1\sigma$. The short-range repulsive potential between ions and beads is given by the same form as the bead-bead repulsive potential in Deserno's model (see eq. (1) in ref. [19]) with $b_{\text{ion-head}} = 0.5\sigma$ and $b_{\text{ion-tail}} = 1.5\sigma$. This choice of parameters allows the ions to approach the surface of the head beads, while excluding them from the hydrophobic core of the bilayer. Electrostatic interactions are computed using Lekner summations [20]. We neglect dielectric discontinuities (*i.e.*, image charges) and assume that all the electrostatic interactions take place in a medium with uniform dielectric constant $\epsilon = 80$, see footnote[1]. The membranes are simulated at zero surface tension using the method described in ref. [22] for fixed-tension implicit-solvent bilayer simulations. Initially, we place a flat membrane with $N/2 = 1000$ lipids per monolayer in the middle of the simulation box, with the counterions distributed evenly above and below the membrane. The system is allowed to equilibrate for 10^5 Monte Carlo (MC) time units, where each time unit τ consists of move attempts to translate and rotate the lipids, ions displacements, and changes in the cross-sectional area of the system. To accelerate the relaxation of the long-wavelength Fourier modes, we also perform a few "mode excitation" moves per τ [23]. After initial thermalization, the systems are simulated for additional $1.8 \times 10^6\tau$, and the quantities of interest are sampled every 50τ. Equilibrium configurations of membranes with charge density $\phi = 0.08$ in solutions of monovalent and pentavalent counterions are displayed in figs. 1(a) and (b), respectively. In the latter case, the ions tend to condense on the membrane, forming a thin Gouy-Chapmann "double layer" [9,10].

Figure 2(a) depicts the spectral intensity (eq. (2)) of the membrane thermal undulations computed for the bilayers with $\phi = 0.08$, whose snapshots are shown in fig. 1. The graphs have been vertically shifted for clarity. Both graphs exhibit the power law $\langle |h_q|^2 \rangle \sim n^{-4}$, in agreement with the form of eq. (2) for $\gamma = 0$. By fitting the simulation results to eq. (2), one can extract the value of κ. Our results are summarized in fig. 2(b), showing κ as a function of ϕ for membranes in solutions of monovalent (circles) and pentavalent (squares) counterions. The dashed line denotes the value of κ for a neutral membrane ($\phi = 0$). We note that the error bars on our measurements of κ are quite large, reflecting not only the difficulty in obtaining good statistics for the spectral intensity of the thermal undulations, but also uncertainties in fitting the data to

[1] It is practically impossible to calculate image charges for a fluctuating surface, which is the reason why they are routinely ignored in simulations of many-particle charged systems. In phospholipid bilayers, the image charges exclude the electric field from the low dielectric hydrophobic core of the membrane. However, we note that the exclusion of the electric field from the membrane is not only a matter of dielectric discontinuities, but can be also attributed to the nearly flat geometry and the charge neutrality on both sides of the membrane. Thus, ignoring dielectric discontinuities may actually be reasonable in some simulations of interfaces. See more detailed discussion in [21].

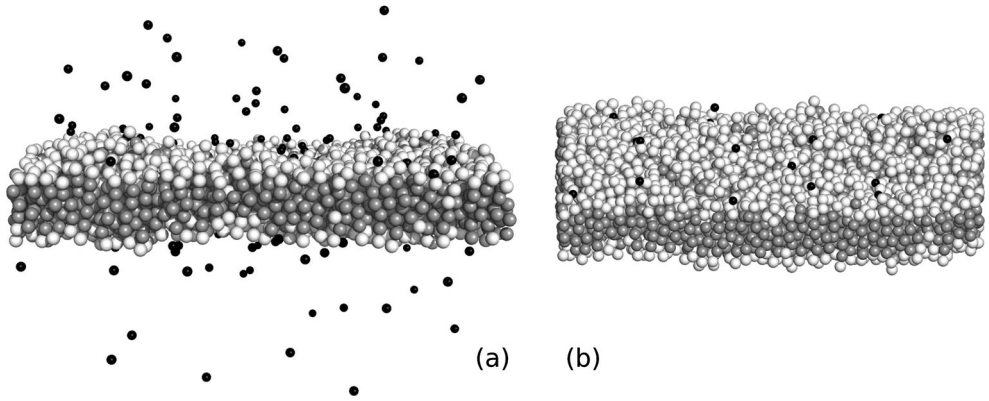

Fig. 1. Equilibrium configurations of membranes with charge density $\phi = 0.08$ in solutions of monovalent (a) and pentavalent (b) counterions. The head and tail beads of the lipids appear in white and gray colors, respectively, while the ions are presented as black spheres.

the functional form of eq. (2). Therefore, it is impossible to draw quantitative conclusions from the data regarding the variations of κ with ϕ. Nevertheless, the data in fig. 2(b) clearly supports the picture that the bending modulus of charged membranes increases from its value for $\phi = 0$ when the counterions are monovalent. This observation is consistent with the PB theory, although it should be acknowledged that previous theoretical calculations of $\delta\kappa$ were done for systems with extra salt and for stationary (non-undulating) membranes [4].

The PB theory is expected to break down when the so-called dimensionless coupling parameter $\Xi = 2\pi Z^3 l_B^2 \phi/a_0$ (where a_0 is the area per lipid and Z denotes the valance of the counterions) becomes much larger than unity. Given the strong dependence of Ξ on Z, it is not surprising that simulations with pentavalent counterions reveal a very different trend of reduction in κ due to electrostatic effects. As in the case of monovelent counterions, the large error bars preclude quantitative analysis of the variation of κ with ϕ. The observation that the bending modulus is reduced when the membrane is charged and suspended in multivalent counterions solution agrees with previous theoretical studies. The fact that the magnitude of the negative electrostatic contribution to κ is fairly small ($\lesssim k_B T$) is also in general agreement with existing theoretical calculations. As discussed in the introduction, the negative electrostatic contribution to κ in pentavalent counterions solutions has been attributed to the attraction due to spatial charge correlations in the double layer, which allows the membrane to bend more easily [8].

The picture emerging from fig. 2 is also consistent with our measurements of the equilibrium projected area per lipid, $a_0 = 2\langle L\rangle^2/N$, depicted in fig. 3. (The prefactor 2 in the definition of a_0 is due to the fact that the number of lipids per monolayer is $N/2$.) In the presence of monovalent counterions, the area per lipid increases linearly with ϕ. The increase in a_0 arises from the *repulsive* electrostatic interactions between the charged lipids, the strength of which is enhanced with the increase in the density ϕ of the charged lipids. The pentavalent counterion simulations feature markedly different behavior, exhibiting a slight decrease in a_0 with ϕ. The decrease in a_0 in this case indicates that the effective electrostatic interactions between the lipids and counterions in the double layer become *attractive* due to spatial charge correlations. Also shown in the figure are results of similar simulations with trivalent counterions which exhibit intermediate behavior between the monovalent and pentavalent counterions. The observed increase in a_0 may be attributed to the fact that the coupling parameter corresponding to the trivalent counterions simulations satisfies $\Xi \lesssim 10$, which is still within the range where, usually, mean-field theory still holds. The same trend of "intermediate" behavior of trivalent counterions is also observed in our results for the bending rigidity (data not shown in fig. 2(b)), in which the electrostatic contribution was found to be vanishingly small.

The increase in area per lipid reported in fig. 3 can be understood as follows: We first note that in the case of no salt, the PB electrostatic free energy $F_{\text{PB-el}} = k_B T \phi N$ (derived by integrating the electrostatic energy density over the entire space) is *independent* of the surface area A. The repulsion arises from the entropy of the counterions which, to an approximation, can be viewed as confined within a volume of size $V = A l_{\text{GC}}$ around the surface, where l_{GC} is the Gouy-Chapmann length. The associated free energy contribution is $F_{\text{PB-en}} \sim -k_B T \phi N \ln(V) = -k_B T \phi N \ln(A^2/N\phi)$, where the last equality is due to the fact that $l_{\text{GC}} \sim (N\phi/A)^{-1}$. Introducing the area per lipid a, and expanding the logarithm around $a^* = a(\phi = 0)$, we find that the area-dependent part of the PB free energy is given by $F_{\text{PB}} = -c k_B T \phi N (a - a^*)/a^*$, where c is a numerical prefactor and the minus sign accounts for the fact that F_{PB} is repulsive. Adding F_{PB} to the elastic energy of the uncharged membrane, yields the following expression for the elastic energy per lipid $f = F/N$:

$$f = \frac{1}{2} K_A \frac{(a - a^*)^2}{a^*} - c k_B T \phi \frac{(a - a^*)}{a^*}\,, \qquad (3)$$

where K_A is the area stretch modulus. This free energy attains a minimum at the area per lipid

$$a_0 = a^* + c\phi(k_B T/K_A), \qquad (4)$$

which grows linearly with ϕ as depicted in fig. 3.

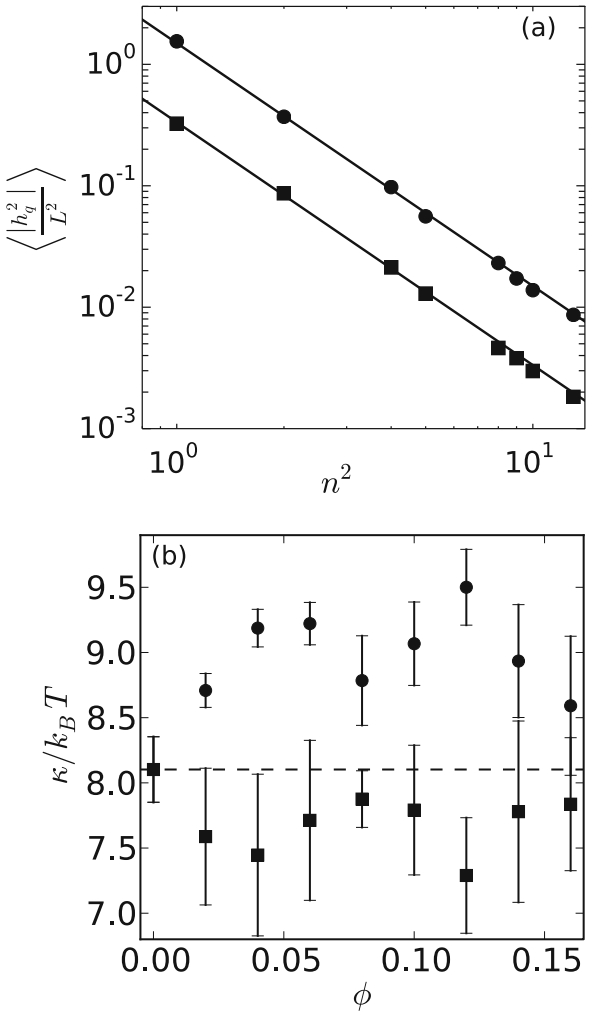

Fig. 2. (a) Spectral intensity as a function the squared wave number n^2. Data has been obtained from simulations of charged membranes with surface charge density $\phi = 0.08$ in solutions of monovalent (circles) and pentavalent (squares) counterions. Solid line indicates a fit to the power law $\langle |h_q|^2 \rangle \sim n^{-4}$ based on the four largest Fourier modes. For clarity, we vertically shifted the graph corresponding to the monovalent counterions simulations, by multiplying the spectral intensities by a factor of 5. (b) The bending rigidity κ as a function of the charge density ϕ for membranes with monovalent (circles) and pentavalent (squares) counterions. Horizontal dashed line indicates the value of κ for neutral membranes ($\phi = 0$).

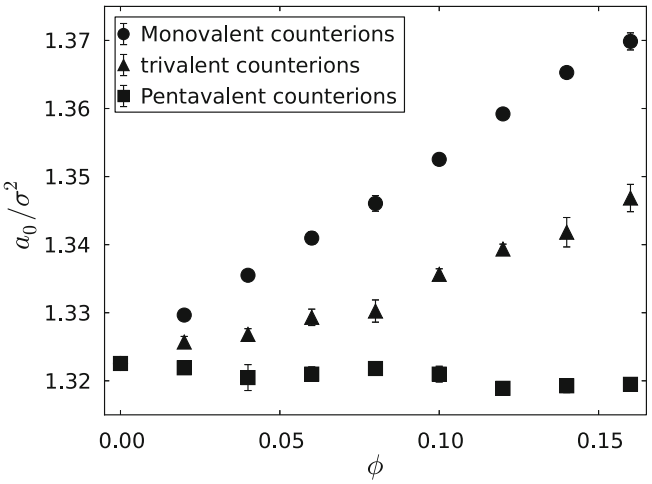

Fig. 3. Projected area per lipid a_0 as a function of ϕ for membranes with monovalent (circles), trivalent (triangles), and pentavalent (squares) counterions.

Interestingly, both experiments [24] and atomistic simulations [25] found the area of monovalently charged phosphatidylserine (PS) lipids to be *smaller* than the area of their neutral phosphattidylcholine (PC) analogs. This counterintuitive result was primarily attributed to the formation of transient intra-molecular hydrogen bonds between the amyne and carboxylate groups of the PS headgroup. Our CG model allows us to "turn off" the hydrogen bonding effect and "isolate" the Coulombic contribution, which turns out to be repulsive in monovalent systems. In our CG simulations, the repulsive electrostatic interactions are balanced by relatively soft hydrophobic interactions. Because of the weakness of these attractive interactions, we observe that for $\phi > 0.16$, the areal strain in the monovalent counterion simulations exceeds the rupture strain of the bilayer membrane, leading to the formation of membrane pores, as demonstrated in fig. 4. The rupture value of ϕ could be increased by including hydrogen bonding in our CG model or, alternatively, by strengthening the hydrophobic interactions, but this will also lead to an undesirable increase in κ. Real PS bilayers have $\kappa \sim 20$–$50 k_BT$ which is several times larger than that of the membrane simulated here. Assuming a linear relationship between the area stretch modulus K_A and bending rigidity κ: $\kappa \sim K_A d^2$, where d is the bilayer thickness [26], we can expect the stretch modulus of real bilayers to also be a few times larger than in simulations. This feature of real PS bilayers, together with the extra attractive interaction provided by the hydrogen bonds, explains their mechanical stability at all charge densities, including for $\phi = 1$. The magnitude of the hydrogen bonding interactions (per lipid) can be roughly estimated by adopting eqs. (3) and (4) derived for the case of repulsive electrostatic interactions, with a modified (negative rather than positive) constant c. For fully charged membrane ($\phi = 1$) PS bilayers, the area stretch modulus is typically $K_A \sim 0.15\,\mathrm{J/m^2}$, and the H-bond interactions reduce the area per lipid from $a^* \sim 0.72\,\mathrm{nm}^2$ to $a_0 \sim 0.65\,\mathrm{nm}^2$ [24]. Substituting these values into eq. (4) yields $c \sim -2.5$. Using this value of c in the second term on the r.h.s. of eq. (3) gives an estimate for the H-bonding free energy contribution which is $f_{\text{H-b}} \sim -0.25 k_BT$.

Pore formation, as exhibited in fig. 4, is not observed when the charged membranes are simulated with pentavalent counterions. Therefore, such membrane can be simulated at much higher values of ϕ. However, the multivalent counterion simulations feature a different type of mechanical instability, which is directly related to the previously discussed reduction in κ. At high charge densities, the membranes in pentavalanet counterion solutions begin to develop large wavelength bending instabilities, as illustrated in the series of snapshots in fig. 5, correspond-

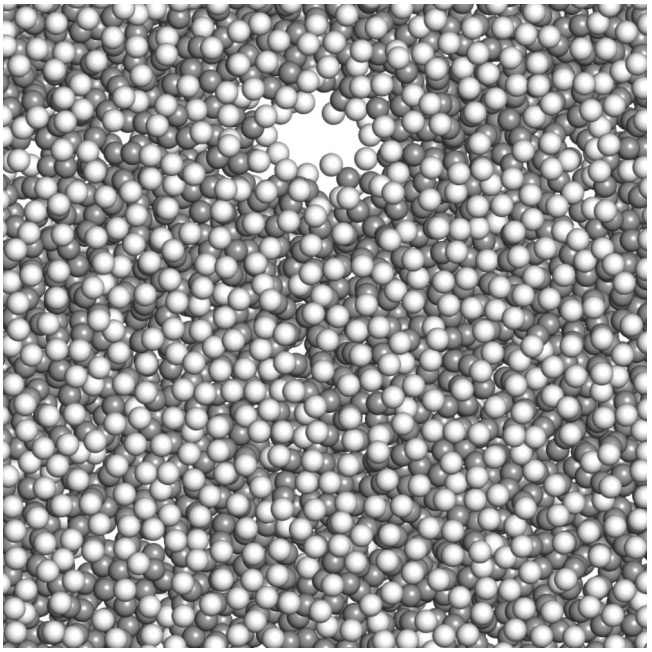

Fig. 4. Top view of a simulated membrane with a pore. The membrane, with charge density $\phi = 0.2$, is in contact with a solution of monovalent counterions (not displayed). Color coding is similar to fig. 1.

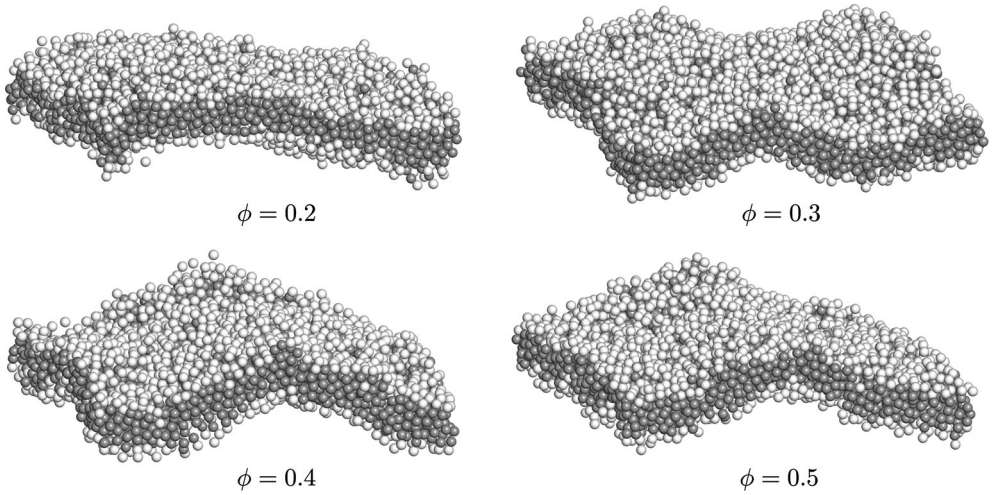

Fig. 5. Sample snapshots of strongly undulating charged bilayers with pentavalent counterions (not displayed). Color coding is similar to fig. 1.

ing to membranes with $0.2 \leq \phi \leq 0.5$. The growth in the amplitude of the undulations, observed in fig. 5, can also be inferred from the results of fig. 6. Here, we plot the spectral intensity of the membranes whose snapshots are displayed in fig. 5. Clearly, there is poor agreement between the results in fig. 6 and eq. (2). The deviation of the computational results from eq. (2) is expected because the power law $\langle |h_q|^2 \rangle \sim n^{-4}$ is derived from the quadratic approximation of eq. (1) which, strictly speaking, is only applicable to weakly fluctuating membranes. The dashed lines represent attempts to fit eq. (2) to the data from the second ($n^2 = 2$) and third ($n^2 = 4$) largest modes. These lines highlight the rapid increase in the undulation amplitude of largest Fourier modes ($n^2 = 1$), which are also the softest modes and the first to become unstable as ϕ increases. The onset of this bending instability can thus be associated with the decline of the "apparent bending modulus" of the first mode, κ_1, which is the value of κ that solves eq. (2) for $n^2 = 1$. The results in fig. 6 correspond to $\kappa_1/k_BT = 5.1 \pm 0.5$, 5.2 ± 0.7, 4.2 ± 0.4, and 3.8 ± 0.4 for $\phi = 0.2$, 0.3, 0.4, and 0.5, respectively. We notice that these values of κ_1 are smaller than the values of κ reported in fig. 2(b) for low charge densities. At even larger charge densities ($\phi > 0.5$), we observe that the undulations continue to grow and ultimately lead to the dissociation of the bilayer membranes.

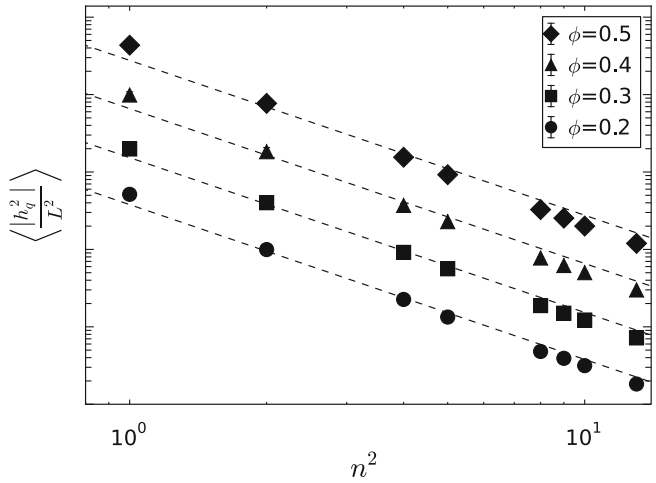

Fig. 6. Spectral intensity of membranes in solutions of multivalent counterions, with surface charge density $\phi = 0.2$ (circles), 0.3 (squares), 0.4 (triangles), and 0.5 (diamonds). Dashed line indicates attempts to fit the data from the second ($n^2 = 2$) and third ($n^2 = 4$) largest modes to the power law form $\langle |h_q|^2 \rangle \sim n^{-4}$. The graphs have been shifted vertically for clarity.

To conclude, we investigated the elastic properties of charged membranes in contact with counterion solutions. The cases of monovalent and multivalent (with $Z = 5$) counterions exhibit distinctly different behaviors. In the former, both the bending rigidity and the equilibrium projected area increase with the membrane charge density. These observations suggest, in agreement with the Poisson-Boltzmann mean-field theory, that the repulsive forces between the lipid charges are only partially screened by the monovalent counterions. In the latter case the trends are opposite, namely both κ and a_0 show a slight decrease with increasing ϕ. These observations can be attributed to the formation of a thin layer of counterions around the membrane, and the fact that the forces between spatially correlated charges within the "double layer" become attractive. More specifically, the presence of multivalent counterions creates regions within the double layer where local charge densities of opposite signs attract each other. The increase in the curvature undulations and decrease in the area per lipid represent mechanisms through which the distances between these correlated regions, especially those residing on the same side of the bilayer, are generally decreased (see illustration in fig. 1 of ref. [6]). The different elastic properties of membranes in monovalent and multivalent solutions lead to different mechanical instabilities. In the former case, pores open to relieve the electrostatic tensile stresses, while the latter case is characterized by a growth in the amplitudes of large wavelength bending modes. As a final note we recall that the elastic properties of real membranes may be affected by other intermolecular forces that can dominate the electrostatic effect on the bending rigidity. Several such "counter mechanisms" have been mentioned in the text, including hydrogen-bonding interactions, screening by salt, ions-lipids excluded-volume interactions, and image charges that weaken the binding of the multivalent counterions to the membrane [27]. The CG simulations provide a framework for systematically exploring the effects of these additional interactions.

This work was supported by the Israel Science Foundation through grant No. 1087/13.

References

1. B. Alberts *et al.*, *Molecular Biology of the Cell* (Garland Science, New York, 2002).
2. W. Helfrich, Z. Naturforsch. **28C**, 693 (1973).
3. O. Farago, P. Pincus, J. Phys. Chem. **120**, 2934 (2004).
4. For a comprehensive review see: D. Andelman, in *Structure and Dynamics of Membranes*, edited by R. Lipowsky, E. Sackmann (Elsevier, Amsterdam, 1995).
5. A.W.C. Lau, P. Pincus, Phys. Rev. Lett. **81**, 1338 (1998).
6. T.T. Nguyen, I. Rouzina, B.I. Shklovskii, Phys. Rev. E **60**, 7032 (1999).
7. R.R. Netz, Phys. Rev. E **64**, 051401 (2001).
8. Y.W. Kim, W. Sung, Europhys. Lett. **58**, 147 (2002).
9. A.W.C. Lau, D.B. Lukatsky, P. Pincus, S.A. Safran, Phys. Rev. E **65**, 051502 (2002).
10. A.G. Moreira, R.R. Netz, Eur. Phys, J. E **8**, 33 (2002).
11. I. Rouzina, V.A. Bloomfield, J. Phys. Chem. **100**, 9977 (1996).
12. N. Grønbech-Jensen, R.J. Mashl, R.F. Bruinsma, W.M. Gelbart, Phys. Rev. Lett. **78**, 2477 (1997).
13. N. Grønbech-Jensen, K.M. Beardmore, P. Pincus, Physica A **261**, 74 (1998).
14. C.C. Fleck, R.R. Netz, Phys. Rev. Lett. **95**, 128101 (2005).
15. E. Lindhal, O. Edholm, Biophys. J. **79**, 426 (2000).
16. S.J. Marrink, A.E. Mark, J. Phys. Chem. **105**, 6122 (2001).
17. O. Farago, J. Chem. Phys. **119**, 596 (2003).
18. F. Brown, Annu. Rev. Phys. Chem. **59**, 685 (2008).
19. I.R. Cooke, K. Kremer, M. Deserno, Phys. Rev. E **72**, 011506 (2005) (we slightly modified the model to avoid occasional escape of lipids from the bilayer).
20. N. Grønbech-Jensen, G. Hummer, K.M. Beardmore, Mol. Phys. **92**, 941 (1997).
21. R.J. Mashl, N. Grønbech-Jensen, J. Chem. Phys. **109**, 4617 (1998).
22. O. Farago, N. Grønbech-Jensen, Biophys. J. **92**, 3228 (2007).
23. O. Farago, J. Chem. Phys. **128**, 184105 (2008).
24. H.I. Petrach, S. Tristram-Nagle, K. Gawrisch, D. Harries, V.A. Persegian, J.F. Nagle, Biophys. J. **86**, 1574 (2004).
25. P. Mukhopadhyay, L. Monticelli, D.P. Tieleman, Biophys. J. **86**, 1601 (2004).
26. W. Rawicz, K.C. Olbrich, T. McIntosh. D. Needham, E. Evans, Biophys. J. **79**, 328 (2000).
27. S. Buyukdagli, M. Manghi, J. Palmeri, Phys. Rev. E **81**, 041601 (2010).